where $R=(Z_A/Z_B)^2(M_B/M_A)$, and it has been assumed that $(y_m/2)^{1-\alpha}\gg 1$.

Taking aluminum antimonide as an example, one finds

$$F_{\mathrm{Sb}}-F_{\mathrm{Al}}=[0.9\ln(E/E_d)-2.5]^{-1}. \quad (28)$$

Evaluations for $E/E_d=10^4$ and 10^5 (which might correspond to $E=0.2$ Mev and 2.0 Mev) give $F_{\mathrm{Sb}}/F_{\mathrm{Al}}=1.4$ and 1.3. Among the primary knockons, Sb atoms are about three times as numerous as Al atoms. The equalizing effect of the fairly long cascades reduces this ratio to the quoted values.

Similar calculations for tungsten carbide show that among the primary knock-ons tungsten atoms are about ten times as numerous as carbon atoms, and that for $E/E_d=10^4$ and 10^5, $F_{\mathrm{W}}/F_{\mathrm{C}}=2.4$ and 1.8. It should be remembered, of course, that these estimates are illustrative. Various factors, such as the excitation of electrons by very fast atoms, have been left out of account.

VII. ACKNOWLEDGMENTS

The author wishes to thank L. W. Aukerman, A. C. Beer, J. H. Cahn, and R. K. Willardson for discussions and for suggestions concerning the preparation of the paper. He is particularly indebted to R. J. Harrison who called attention to several mathematical points during the course of the work and made a critical review of the manuscript.

PHYSICAL REVIEW VOLUME 112, NUMBER 5 DECEMBER 1, 1958

Nuclear Magnetic Resonance in Cerous Magnesium Nitrate at Temperatures below 1°K*

T. L. Estle, H. R. Hart, Jr., and J. C. Wheatley
Department of Physics, University of Illinois, Urbana, Illinois

(Received June 2, 1958)

The nuclear resonance of the protons in cerous magnesium nitrate, $Ce_2Mg_3(NO_3)_{12}\cdot 24H_2O$, has been studied in a single crystal cooled to temperatures below 1°K by partial adiabatic demagnetization and adiabatic rotation. The area under the nuclear resonance was used as a thermometric parameter. The area did not obey Curie's law as a result of the temperature-dependent local rf field. A $T-T^*$ relation was derived which gave temperature ratios on adiabatic rotation which agreed within 5–10% with ratios calculated from the properties of the crystal. The lowest measured temperature was 5×10^{-3}°K.

A study of the structure of the resonance showed that the splittings were caused by the average magnetization of the cerium ions and that the protons were at least 5 A from the cerium ions.

I. INTRODUCTION

a. Adiabatic Rotational Cooling

MANY paramagnetic crystals can be cooled to temperatures below 1°K by the well-known techniques of adiabatic demagnetization.[1–3] An alternative process, adiabatic rotational cooling, can be applied to crystals with an appreciable magnetic anisotropy.[4–10] Rotational cooling achieves the necessary reduction in the energy between the magnetic substates of the ion in a magnetic field by changing the relative orientation of the field and the crystal. In adiabatic demagnetization the energy splitting is reduced by reducing the magnetic field applied to the crystal. In the present experiments both techniques have been employed, the rotational cooling being preceded by a reduction of the magnetic field.

Consider an idealized paramagnetic crystal in which the interactions of a given ion with other paramagnetic ions and with the moment of its own nucleus are negligible. Let us assume that there is only one type of magnetic ion and that the crystalline electric field has split the free-ion energy levels so that only a Kramers doublet lies low enough to be appreciably populated at temperatures near 1°K. It follows from the Boltzmann expression for the relative populations of the two levels, that the magnetic energy splitting of the ground doublet divided by the absolute temperature, T, is a constant for all isentropic processes. Hence, for isentropic

* This work was supported by the joint program of the Office of Naval Research and the U. S. Atomic Energy Commission. It is based on a thesis submitted by T.L.E. in partial fulfillment of the requirements for the Ph.D. degree, University of Illinois.

[1] E. Ambler and R. P. Hudson, *Reports on Progress in Physics* (The Physical Society, London, 1955), Vol. 18, p. 251.

[2] D. de Klerk and M. J. Steenland, *Progress in Low-Temperature Physics*, edited by J. C. Gorter (North-Holland Publishing Company, Amsterdam, 1955), Vol. 1, p. 273.

[3] D. de Klerk, *Handbuch der Physik* (Springer-Verlag, Berlin, 1956), Vol. 15, p. 38.

[4] Bogle, Cooke, and Whitley, Proc. Phys. Soc. (London) **A64**, 931 (1951).

[5] J. W. T. Dabbs and L. D. Roberts, Phys. Rev. **95**, 307 (1954).

[6] Cooke, Whitley, and Wolf, Proc. Phys. Soc. (London) **A68**, 415 (1955).

[7] J. C. Wheatley and T. L. Estle, Phys. Rev. **104**, 264 (1956).

[8] Hart, Estle, and Wheatley, *Low Temperature Physics and Chemistry*, edited by J. R. Dillinger (University of Wisconsin Press, Madison, 1958), p. 562.

[9] Estle, Hart, and Wheatley, *Low Temperature Physics and Chemistry*, edited by J. R. Dillinger (University of Wisconsin Press, Madison, 1958), p. 204.

[10] T. L. Estle, thesis, University of Illinois, 1957 (unpublished).

processes the variation of T is given by

$$T \propto gH, \tag{1}$$

where H is the magnetic field and g is the spectroscopic splitting factor. In general g depends on the relative orientation of the crystalline axes and the magnetic field. In the case of axial symmetry, g has two principal values $g_{\parallel}$ and $g_{\perp}$ respectively parallel and perpendicular to the axis. In this case g is given by

$$g=(g_{\parallel}^2\cos^2\theta+g_{\perp}^2\sin^2\theta)^{\frac{1}{2}}, \tag{2}$$

where θ is the angle between the magnetic field and the crystalline axis. The simplest form of the equation basic to rotational cooling, the relation of T to θ on an isentrope, takes the form

$$T(\theta)=T(\pi/2)g_{\perp}^{-1}(g_{\parallel}^2\cos^2\theta+g_{\perp}^2\sin^2\theta)^{\frac{1}{2}} \tag{3}$$

for axial symmetry.

Cerium magnesium nitrate, $Ce_2Mg_3(NO_3)_{12}\cdot 24H_2O$, is an excellent paramagnetic crystal for use in rotational cooling experiments.[7,11,12] The general features of rotational cooling have been confirmed for this crystal[7] by observing the variation of the temperature, calculated from ballistic adiabatic susceptibility measurements, with the angle θ. These experiments show that CMN does indeed exhibit the above properties of the idealized axially symmetric paramagnetic crystal over a wide range of temperature and magnetic field. The ballistic measurements yield a lower limit of 57 for the ratio $g_{\perp}/g_{\parallel}$, in disagreement with earlier measurements.[13] Since the value of $g_{\perp}$ has been determined by paramagnetic resonance to be 1.84 ± 0.02,[13] the value $g_{\parallel}$ is not greater than 0.03. Only at very low temperatures or rather low magnetic fields do the effects of interionic interactions become appreciable.

b. Nuclear Magnetic Resonance[14]

Since CMN contains waters of hydration, a strong NMR signal from the protons should be attainable. This signal in a crystal cooled below 1°K might serve as a useful thermometric parameter. The intensity of the NMR absorption is proportional to the difference in populations of the two nuclear magnetic substates which is in turn proportional to $\Delta W/kT$, where ΔW, the energy separation of the two substates, is assumed to be much less than kT. The absorption is also proportional to H_1^2, where $2H_1$ is the component of the rf magnetic field acting on the protons which is perpendicular to the static magnetic field. For narrow lines these two are the only important factors. If H_1 is independent of T, and if saturation of the resonance does not occur, the area under the absorption curve may be used as a thermometric parameter and will be proportional to $1/T$ for narrow lines. Narrow lines are found in crystals containing no paramagnetic ions. However, the spin-lattice relaxation time is very long in such crystals at low temperatures so that very low rf levels would be required in order to avoid saturation. The spin-lattice relaxation time for protons in nonparamagnetic crystals has been found to be in the neighborhood of 10^2 to 10^4 seconds at liquid helium temperatures and the relaxation time increases rapidly with decreasing T.[15,16] Paramagnetic crystals on the other hand have rather short spin-lattice relaxation times even at 1°K.[15] Hence, the temperature of the proton spin system is equal to that of the rest of the crystal for much higher power levels than could be used with nonparamagnetic crystals. However, apart from considerations of saturation, the interpretation of NMR in a paramagnetic crystal at low temperatures is not as simple as it would be in a nonparamagnetic crystal. The paramagnetic ions produce magnetic fields which in turn profoundly influence the nuclear spin system. A static local field produced by the paramagnetic ions adds to the applied magnetic field and gives the resonance line a structure because of the many nonequivalent proton sites.[17,18] In addition, at the frequencies used a component of the magnetization of the cerium ions follows the applied rf field and results in a temperature-dependent local rf field.

If one wishes to use the total area under the absorption curve as a thermometric parameter, then the interpretation of this area in terms of temperature is complicated not only by the temperature-dependent H_1 but also by the fact that the external parameters, either field or frequency, have to be varied in order to obtain the complete NMR lines. If quantities referring to one of the N_p proton sites are designated by the subscript i $(i=1,\cdots,N_p)$, then the total energy ΔE absorbed in traversing the resonance, using field sweep at constant temperature, will be

$$\Delta E=\left(\frac{dH}{dt}\right)^{-1}\frac{\gamma^3\hbar^2}{16\pi k}\frac{H_0^2}{T}\sum_i H_{1i}^2(T). \tag{4}$$

For a field sweep with H/T constant, one finds

$$\Delta E=\left(\frac{dH}{dt}\right)^{-1}\frac{\gamma^3\hbar^2}{16\pi k}\frac{H_0^2}{T_0}\sum_i\Bigg\{H_{1i}^2(T_0)+\frac{\delta H_i(H_0,T_0,\theta)}{H_0}\left[H_{1i}^2(T_0)-T_0\frac{dH_{1i}^2(T_0)}{dT}\right]+\left(\frac{\delta H_i(H_0,T_0,\theta)}{H_0}\right)^2\left[H_{1i}^2(T_0)-T_0\frac{dH_{1i}^2(T_0)}{dT}+\tfrac{1}{2}T_0^2\frac{d^2H_{1i}^2(T_0)}{dT^2}\right]+\cdots\Bigg\}, \tag{5}$$

[11] Cerium magnesium nitrate will hereafter be denoted by CMN.
[12] J. M. Daniels and F. N. H. Robinson, Phil. Mag. 44, 630 (1953).
[13] Cooke, Duffus, and Wolf, Phil. Mag. 44, 623 (1953).
[14] Nuclear magnetic resonance will hereafter be denoted by NMR.
[15] N. Bloembergen, Physica 15, 386 (1949).
[16] J. Hatton and B. V. Rollin, Proc. Roy. Soc. (London) A199, 222 (1949).
[17] N. Bloembergen, Physica 16, 95 (1950).
[18] N. J. Poulis, Physica 17, 392 (1951).

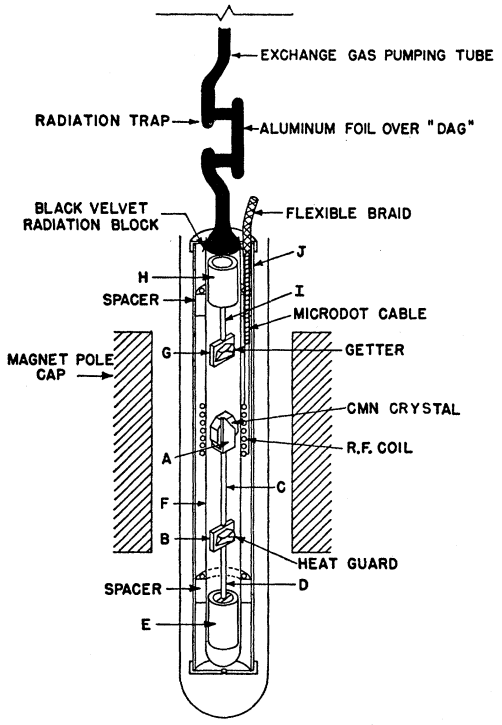

FIG. 1. Schematic diagram of NMR probe and crystal holder. *A*, *B*, and *G* are glass plates. *C*, *D*, and *I* are thin-walled glass tubes. *E* and *H* are glass cylinders which slide inside glass tube *F*. *J* is a copper shield.

while for a frequency sweep, one finds

$$\Delta E=\left(\frac{d\nu}{dt}\right)^{-1}\frac{\gamma^4\hbar^2}{32\pi^2k}\frac{H_0^2}{T}\sum_i\left\{H_{1i}^2(T)\left[1+2\frac{\delta H_i(H_0,T_0,\theta)}{H_0}+\left(\frac{\delta H_i(H_0,T_0,\theta)}{H_0}\right)^2\right]\right\}. \quad (6)$$

In Eqs. (4), (5), and (6), δH_i is the component parallel to the strong field of the static magnetic field produced by the cerium ions at site i, and H_{1i} is one-half the component normal to the external field of the rf field at the ith site. The subscripts 0 indicate quantities related by the free proton resonance condition, $\nu_0=(\gamma/2\pi)H_0$. In Eq. (5) T_0 is the temperature when the external field is H_0. The quantities γ, $\hbar$, and k are the gyromagnetic ratio of the proton, Planck's constant, and the Boltzmann constant, respectively. Equation (4), besides being applicable in ordinary isothermal experiments, is valid in adiabatic experiments in which the crystal temperature is independent of the external magnetic field. Equation (5) is applicable to adiabatic experiments in which the interaction of the paramagnetic ions with the external field is large enough so that T varies linearly with H. Equation (6) gives the results of an attempt to maintain constant crystal temperature in adiabatic experiments by varying the frequency. However, differences in the population ratios of the magnetic substates of nonequivalent protons complicate the interpretation of the results in both adiabatic and isothermal experiments. There is no obvious advantage to be obtained by employing a frequency sweep, so that the experimentally simpler sweep of the magnetic field was used in the experiments to be described in this paper. Equations (4), (5), and (6) also include the possibility of a temperature-dependent local rf field.

II. EXPERIMENTAL METHOD

a. Apparatus

A clear, 2.8-g CMN crystal cut from a larger crystal was used in the experiments. It was about 2.9 cm long, 1.3 cm wide, and 4.35 mm thick. The crystal was not ellipsoidal although the corners were all rounded off and there were no regions of the surface which were concave outward. The Curie-Weiss delta, 2.5×10^{-3}°K obtained by adiabatic demagnetization using ballistic susceptibility measurements is consistent with the value, 2.7×10^{-3}°K, calculated for an ellipsoid having the above axes.[19]

The experimental arrangement is shown in Fig. 1, all glass parts being made from Pyrex. The CMN crystal was sandwiched between two glass plates, *A*, so that the trigonal crystalline axis was normal to the plates and thus horizontal. It was secured by gluing it to the glass with G.E. 7031-toluene varnish.[20] The glass plates holding the CMN crystal were connected to a second glass plate, *B*, 10 cm below by means of glass tubing, *C*, about 3 mm in diameter with a $\frac{1}{4}$-mm wall. Glued on to plate *B* were five single crystals of ferric alum, $Fe(NH_4)(SO_4)_2\cdot12H_2O$, of total mass 2 g which, when cooled, served to reduce the solid conduction heat leak. Plate *B* was connected by similar glass tubing, *D*, 2 cm long, to the glass cylinder, *E*, which was glued into the 25-mm glass sample tube, *F*. The tubes *C* and *D* were made large in order to resist the rather large torques acting on the crystal when the magnetization is not colinear with the field. Seventeen cm above the CMN crystal, 8 ferric alum crystals of total mass 4 g were glued to the glass plate, *G*, which was suspended from the glass cylinder, *H*, by another thin-walled glass tube, *I*. The purpose of this group of crystals, called the getter, was to adsorb residual helium exchange gas. Accordingly, the getter could be cooled prior to the reduction of the field by being raised into the fringing field of the magnet. The sample tube, *F*, was connected through a radiation trap and a 6-mm exchange gas pumping tube to the exchange gas handling system. The sample tube, *F*, was completely shielded to prevent radiation heat input. These techniques are developments of those described in reference 20. This crystal mount was used in all of the experiments discussed later. The angle between the trigonal axis and the

[19] J. A. Osborn, Phys. Rev. **67**, 351 (1945).
[20] Wheatley, Griffing, and Estle, Rev. Sci. Instr. **27**, 1070 (1956).

strong magnetic field was varied by rotating the exchange gas pumping tube from the top of the cryostat.

Two different arrangements were used for shielding the crystal from radiation. The first, used in experiment A to be described later, yielded a spurious signal from extraneous hydrogenous material (paper, Formex, glue) which complicated the interpretation of the results. The second arrangement, used in experiment B, eliminated the spurious signal. In experiment B the trap and the top of the sample tube were covered first with colloidal graphite in alcohol (Dag) and then with aluminum foil. The sample tube was enclosed in the copper shield can, J. In order to allow circulation of liquid helium through the can, there was a hole in the bottom and a loose fit at the top. Care was taken to trap radiation entering through these openings. This copper can rotated with the sample tube.

The 4 cm long coil which produced the rf field, H_1, contained 12 turns of number-16 bare copper wire directly in contact with the sample tube. The cable connecting the coil to the external electronic equipment was one continuous piece of 50-ohm Microdot cable.[21] It had Teflon insulation between the inner conductor and the shield and was covered with a nylon jacket. This small cable offered a reasonable compromise between low heat input to the helium, flexibility, and low attenuation of the rf signal. Since the cable contained nylon and Teflon it was terminated outside the region of large magnetic field, the connection to the coil being made by two pieces of glass-insulated copper wire. The coil and the coaxial cable were enclosed in a noncurrent-carrying shield, grounded at the receiver only, in order to minimize the effects of external disturbances on the rf voltage. This shield consisted of the copper can, J, about 15 cm of a fine flexible braid directly above J, and a sealed-off double-walled section of cupro-nickel tubing which led to the top of the cryostat. This double-walled section reduced the thermal effects on the electrical characteristics of the cable of the cold helium gas flowing up the cryostat.

The electrical apparatus used in the experiment is shown in block diagram in Fig. 2. The magnet employed was a Varian Model V-4012 electromagnet with a 2.84-inch pole gap and 11.9-inch diameter pole pieces. The magnetic field was swept linearly through the region of the resonance, and a 30-cps modulation was superposed. The battery-powered rf oscillator fed the tuned circuit through a high-impedance capacitor, C_1 ($\sim 1\ \mu\mu$f). The tuned circuit consisted of the rf coil and connecting cable described above and an external variable air-capacitor, C, which could be varied between 20 and 50 $\mu\mu$f. The cable produced a considerable modification to a simple L-C circuit since it had a capacitance of 27.9 $\mu\mu$f/ft, a total inductance comparable to that of the coil, and a resistance larger than any other resistances in the tuned circuit. The Q of the

[21] Microdot Incorporated, 1826 Fremont Avenue, South Pasadena, California.

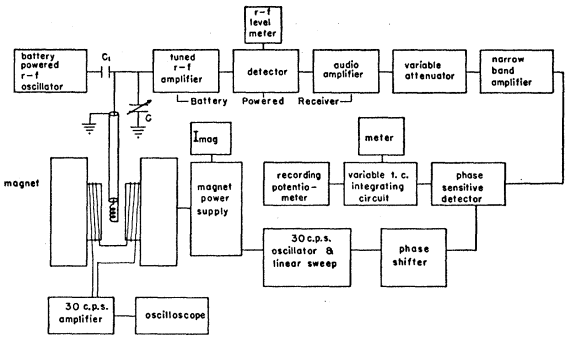

FIG. 2. Block diagram of NMR apparatus.

rf coil, shield, and connecting cable was approximately 10 to 15 as measured by a "Q" meter. The rf amplifier consisted of two tuned-plate stages each having a gain of about 40. The second stage fed a diode detector. The output of the detector was measured and assumed to be proportional to the average rf level at the tuned circuit. The 30-cps component of the envelope was then amplified and in turn detected by a mercury-relay operated "lock-in" detector. The band width was determined by an integrating circuit which followed the "lock-in." The output of the integrating circuit was recorded by a recording potentiometer.

b. Cooling Cycle

The cooling cycle differed from the one used in most adiabatic demagnetization experiments in that the magnetic field was not reduced to zero but instead was reduced to the resonance value. The resonance field was determined by the following considerations. The NMR sensitivity increases as the resonance field increases. However, in order to substantially reduce the heat input from the residual helium heat exchange gas, it is necessary to reduce the crystal temperature to $\frac{1}{4}$°K or below so that the residual gas will be adsorbed. Since the crystal temperature is proportional to the applied field for an adiabatic process, the field must be reduced by at least a factor 4 from the value of the field during the isothermal magnetization part of the cycle in order to reduce the gaseous heat input substantially. On this basis the resonance field was chosen in the region of 2.5 kg. Some decrease in the gaseous heat input was also provided by the getter crystals, Fig. 1. Just prior to demagnetization the cryostat was raised, these crystals being moved into the fringing field. The getter cooled and adsorbed a significant amount of residual heat exchange gas.

The residual heat input to the crystal was normally between 10 and 20 erg/min. Although an rf field $2H_1$ of 4.8×10^{-3} gauss seemed to increase the heat input at the lowest temperatures significantly over the residual value, reduction of $2H_1$ to 2.2×10^{-3} gauss apparently reduced the heat input to the residual value. It is probable that solid conduction contributed to the

residual heat input as a result of the large size glass tube and the higher than normal temperature of the heat guard crystals.

III. CIRCUIT ANALYSIS

For purposes of circuit analysis the rf oscillator in Fig. 2 is replaced by a constant voltage source of magnitude V_0 and angular frequency ω feeding the tuned circuit through the high-impedance capacitor C_1. The external tuning capacitance is C and the voltage at the input to the rf amplifier is V. The coil has inductance L and resistance R, including paramagnetic effects, and distributed capacitance C_d. The coil is connected to the capacitor by a cable having characteristics c, l, and r, per unit length and a length s ($\sim\lambda/15$). If one uses the condition that the circuit be tuned to maximum $|V|$ in the absence of a nuclear signal, one obtains the following approximate expression for $|V|$:

$$|V| = V_0\omega C_1\frac{b_0^2}{a_0}\left[1-\frac{(1+\omega^2 s^2 lc)}{a_0[1-\omega^2 L_0(sc+C_d)]^2}\Delta R\right], \quad (7)$$

where

$$a_0=\frac{R_0(1+\omega^2 s^2 lc)+sr(1-\omega^2 L_0 C_d)[1-\omega^2 L_0(sc+C_d)]}{[1-\omega^2 L_0(sc+C_d)]^2},$$

$$b_0=\frac{\omega L_0+\omega sl(1-\omega^2 L_0 C_d)}{1-\omega^2 L_0(sc+C_d)}, \quad \Delta R=4\pi\omega L_0\zeta\chi'',$$

and R_0, L_0, ζ, and χ'' are, respectively, the resistance and self-inductance of the coil in the absence of a resonance, the filling factor, and the imaginary part of the nuclear susceptibility. In Eq. (7) the squares of resistances are neglected compared to the squares of reactances, and the dispersion is neglected compared to the absorption. One can neglect the effects of dispersion on $|V|$ if one has $a_0 \ll b_0$, i.e., a large Q. Measurements of Q indicate that $(b_0/a_0)\cong 10$ and thus that the effects of dispersion on $|V|$ are not entirely negligible in these experiments. However, since to a first approximation the dispersion does not affect the area under the absorption curve, it can be neglected. It is also assumed that the electronic dispersion and absorption do not change in the region of magnetic fields traversed in obtaining the resonances.

The change in voltage $|\Delta V| = |V(\Delta R)| - |V(\Delta R = 0)|$ is the nuclear signal. The integral $\int|\Delta V|dH$ is proportional to the total energy absorbed by the nuclei when the resonance is traversed and hence is proportional to the energies given in Eqs. (4) and (5).

It was found empirically that as the level of the liquid helium dropped in the Dewar, the rf voltage at the detector dropped without a large detuning of the resonant circuit. Also, at very low temperatures it was found that paramagnetic absorption produced a very large change in the detected rf level without a concomitant large detuning. Thus it appeared that the changes in the circuit parameters during an experiment were primarily resistive.

It is important to note that all resistive elements enter Eq. (7) through a_0. Hence, if a thermometric parameter independent of resistance variations is to be obtained, a quantity independent of a_0 must be employed. Such a quantity is $|V(\Delta R=0)|^2[\int|\Delta V|dH]^{-1}$. The thermometric parameter used to interpret these experiments is inversely proportional to the area under a nuclear absorption curve divided by the square of the rf level measured in the absence of a nuclear signal.

Some evidence for the quadratic rf level correction to the nuclear resonance areas to obtain a thermometric parameter was obtained by analyzing the results of a calibration of the nuclear resonance thermometer against the vapor pressure of helium. The results are presented in Table I. The rf level dropped during the calibration as a result of the decreasing level of the liquid helium. As a result the areas were not strictly proportional to $1/T$, as is shown in the second column. However, a thermometric parameter inversely proportional to Area/V_{rf}^2 showed no systematic variations over the helium temperature range.

TABLE I. The quantity ATV_{rf}^n is given as a function of the temperature determined from the helium vapor pressure. The radio-frequency voltage at the detector, V_{rf}, changes with both temperature and helium level. A is the nuclear resonance area, uncorrected for changes in the rf level at the coil. The quantity AV_{rf}^{-2} follows Curie's law with highest accuracy.

T(°K)	ATV_{rf}^0	ATV_{rf}^{-1}	ATV_{rf}^{-2}	ATV_{rf}^{-3}
4.178	1.000	1.000	1.000	1.000
3.504	1.013	1.016	0.997	0.990
2.996	1.060	1.048	1.037	1.029
2.520	1.060	1.049	1.037	1.025
2.069	1.091	1.046	1.000	0.963
1.845	1.133	1.070	1.013	0.956
1.515	1.133	1.060	0.990	0.928

IV. EXPERIMENTS

Initial experiments at 30 Mc/sec showed an increase of nuclear absorption on adiabatic rotation. Considerable structure was exhibited with a maximum width of the order of 100 gauss. The relative cooling obtained appeared to be comparable with that inferred from ballistic susceptibility measurements. The major difficulty was a large gaseous heat leak which resulted because the resonance field of 7000 gauss was too large to permit efficient adsorption of the residual helium exchange gas (see Sec. II b). All subsequent experiments were performed at fields in the region of 2500 gauss, which corresponds to a resonance frequency of about 10 Mc/sec.

In experiment A, made at a frequency of 10 Mc/sec, there was a spurious signal from extraneous hydrogenous material superposed on the signal from the CMN crystal. The spurious signal was 11 or 12 gauss wide and 9 times as intense as the signal from the CMN when both corresponded to the same tempera-

ture. The extraneous hydrogeneous material was apparently in contact with the liquid helium bath since the intensity of the spurious signal corresponded to the bath temperature except for periods of time after the magnetic field was changed, when it decreased exponentially to the bath temperature intensity with a time constant of about 1.7 minutes. It was possible to correct for the spurious signal by subtracting its area from the total area. In experiment B, made at a frequency of 10.921 Mc/sec, no spurious signal could be detected.

In all experiments the recorder plotted the derivative of the absorption curve, so that double integration was necessary in order to obtain the area under the absorption curve. The double integration was done numerically as indicated in the Appendix.

In order to obtain a thermometric parameter from the absorption curves it was also necessary to measure the rf level, the linear sweep rate, and the amplitude of the 30 cps modulation, which was typically $7\frac{1}{4}$ gauss peak to peak. The time taken to sweep through the resonance varied from 100 to 700 seconds.

V. RESULTS AND DISCUSSION—TEMPERATURES

a. T-T^* Relation

The principal contributions to the deviations of NMR areas from a $1/T$ temperature dependence result from the effects of the paramagnetic ions. The paramagnetic ions may broaden the line to such an extent that the area is not proportional to $1/T_0$, T_0 being the temperature at the free proton resonance field. Also, the local rf field at a proton site may be temperature dependent. The broadening effect is not large in CMN, but the temperature variation of the local rf field profoundly influences the results. The variation with temperature of the local rf field may be estimated as follows. It is assumed that the z-axis is fixed parallel to $g_{\parallel}$, that the strong field rotates in the x-z plane, and that the oscillating field is directed along the y-axis. The local rf field, $\mathbf{H}_{1i}$, acting on a proton occupying a site labeled by the subscript i, produced by the external rf field, $\mathbf{H}_1$, and by the cerium ions at sites labeled by the index j, is given by

$$\mathbf{H}_{1i}=\mathbf{H}_1+\frac{\Delta}{C_\perp}\mathbf{M}_1-\sum_j\left(\frac{\mathbf{M}_1}{N}\frac{1}{r_{ij}^3}-\frac{3\mathbf{r}_{ij}}{r_{ij}^5}\left(\frac{\mathbf{M}_1}{N}\cdot\mathbf{r}_{ij}\right)\right), \quad (8)$$

where $\mathbf{r}_{ij}$ is a vector from the ith proton site to the jth cerium ion, $2\mathbf{M}_1$ is the rf magnetization of the cerium ions, N is the number of cerium ions per unit volume, Δ is the Curie-Weiss delta in the direction of $\mathbf{H}_1$, $C_\perp$ is the perpendicular Curie constant, and the sum over j is carried out within a sphere surrounding the ith proton. $\mathbf{M}_1$ is assumed to be along $\mathbf{H}_1$ and perpendicular to the strong field.

The total energy absorbed in traversing a resonance is proportional to $\sum_i H_{1i\perp}^2$ where i is summed over the N_p protons in the crystal and $H_{1i\perp}$ is the component of the local rf field perpendicular to the static local field. Hence the total energy absorbed will be proportional to a mean square perpendicular local field defined by

$$\langle H_{1\mathrm{loc}}^2\rangle\equiv\frac{1}{N_p}\sum_i H_{1i\perp}^2. \quad (9)$$

In terms of the local field defined by Eq. (8) one finds after some calculation

$$\langle H_{1\mathrm{loc}}^2\rangle=H_1^2+2H_1M_1\frac{\Delta-\delta_1}{C_\perp}+\frac{M_1^2}{C_\perp^2}[\Delta^2-2\Delta\delta_1+\delta_2^2+\delta_3^2\cos^2\theta-2\delta_4^2\sin\theta\cos\theta+\delta_5^2\sin^2\theta], \quad (10)$$

where θ is the angle between the strong field and the z-axis, and where the δ's are given by

$$\begin{aligned}
\delta_1&=\frac{C_\perp}{N_pN}\sum_{i,j}\frac{r_{ij}^2-3y_{ij}^2}{r_{ij}^5},\\
\delta_2^2&=\frac{C_\perp^2}{N_pN^2}\sum_{i,j,k}\frac{(r_{ij}^2-3y_{ij}^2)(r_{ik}^2-3y_{ik}^2)}{r_{ij}^5r_{ik}^5},\\
\delta_3^2&=9\frac{C_\perp^2}{N_pN^2}\sum_{i,j,k}\frac{x_{ij}y_{ij}x_{ik}y_{ik}}{r_{ij}^5r_{ik}^5},\\
\delta_4^2&=9\frac{C_\perp^2}{N_pN^2}\sum_{i,j,k}\frac{x_{ij}y_{ij}y_{ik}z_{ik}}{r_{ij}^5r_{ik}^5},\\
\delta_5^2&=9\frac{C_\perp^2}{N_pN^2}\sum_{i,j,k}\frac{y_{ij}z_{ij}y_{ik}z_{ik}}{r_{ij}^5r_{ik}^5}.
\end{aligned} \quad (11)$$

In Eqs. (11) the indices j and k are summed over the cerium ion sites in a sphere around a proton, and the index i is summed over all the protons in the crystal. If the protons are distributed with spherical symmetry around a cerium ion, then one has $\delta_1=0$, $\delta_4^2=0$, and $\delta_3^2=\delta_5^2$. It seems likely in CMN that the proton distribution about a cerium ion approximates spherical symmetry, so that as a first approximation we will assume that the mean square perpendicular local field has the form

$$\langle H_{1\mathrm{loc}}^2\rangle=H_1^2+2H_1M_1\frac{\Delta}{C_\perp}+\frac{M_1^2}{C_\perp^2}(\Delta^2+\delta^2), \quad (12)$$

where

$$\delta^2=\delta_2^2+\delta_3^2=\delta_2^2+\delta_5^2.$$

If the static magnetization is perpendicular to $\mathbf{H}_1$, the changes of magnetization along $\mathbf{H}_1$ for given changes in $\mathbf{H}_1$ will be the same for either adiabatic or isothermal processes. Hence, neglecting saturation of the static cerium magnetization, at these frequencies $\mathbf{M}_1$ will be related to $\mathbf{H}_1$ by the zero-frequency susceptibility, so

that one has

$$\mathbf{M}_1=\left(\frac{C_\perp}{T-\Delta}\right)\mathbf{H}_1. \tag{13}$$

In this case the mean square perpendicular local field may be written

$$\langle H_{1\mathrm{loc}}^2\rangle=H_1^2\frac{T^2+\delta^2}{(T-\Delta)^2}. \tag{14}$$

Equations (13) and (14) will be modified in the event that the adiabatic and isothermal paramagnetic susceptibilities are not equal to one another. If the crystalline g_{11}-direction does not lie precisely in the plane of rotation of the magnetic field, it is possible for small angles θ that the static magnetization will rotate into the direction of $\mathbf{H}_1$. In this case, provided the external field interaction is large compared with interionic interactions, the adiabatic paramagnetic susceptibility becomes zero and one has $\langle H_{1\mathrm{loc}}^2\rangle=H_1^2$. In practice, the rf magnetization M_1 will lie somewhere between zero and the value given by Eq. (13), its actual value depending in detail on the misalignment angle, the value of g_{11}, and the coefficient of $1/T^2$ in the interionic interaction entropy. The experimental data are not accurate enough to distinguish the effects of finite g_{11} and misalignment at low angles θ. In general, the effect of misalignment is to reduce $\langle H_{1\mathrm{loc}}^2\rangle$ from the value given by Eq. (14).

One may define a thermometric parameter T^* to be inversely proportional to the area under an NMR absorption curve which has been corrected to a standard value for H_1 by dividing the area by the square of the rf level. Since the corrected area is proportional to $\langle H_{1\mathrm{loc}}^2\rangle/T$, the most convenient explicit form for T^* is obtained by defining T^* by the equation $H_1^2/T^*\equiv\langle H_{1\mathrm{loc}}^2\rangle/T$. Then Eqs. (14) yields the $T-T^*$ relation

$$T^*=T(T-\Delta)^2/(T^2+\delta^2). \tag{15}$$

Hence T^* is equal to T at high temperatures. The effect of misalignment, for a given T^*, is to reduce the value of T from that value calculated from Eq. (15).

TABLE II. Experimental and calculated data for the lowest measured temperatures. The numbers in a given row correspond to the same entropy. T is calculated from T^* by means of Eq. (15) with $\Delta=2.5\times10^{-3}$°K and $\delta=7.0\times10^{-3}$°K.

θ (degrees)	$T_{9.8°}$ (10^{-3}°K)	T_θ^* (10^{-3}°K)	T_θ (10^{-3}°K)	$T_{90°}/T_\theta$
0.0	47.3	0.835	5.92	47.0
0.0	47.9	0.849	5.93	47.5
0.0	49.9	0.950	6.15	47.6
0.0	48.7	0.982	6.21	46.1
0.2	50.5	1.025	6.30	47.1
0.0	47.6	1.100	6.43	43.6
0.2	53.3	1.197	6.60	47.5
0.0	55.9	1.264	6.71	48.9
0.0	51.5	1.292	6.75	44.9
0.0	53.7	1.292	6.75	46.7
0.2	56.0	1.370	6.88	47.9
0.2	50.2	1.389	6.90	42.8

TABLE III. Averaged results for the ratio of the temperature at 90°, $T_{90°}$ to that at 0°, $T_{0°}$ on adiabatic rotation.

$T_{9.8°}$ (10^{-3}°K)	$T_{90°}/T_{0°}$	Number averaged
55	46.9	21
76	45.8	9
96	49.5	5
114	49.4	4
133	43.7	3

(b) Experiment *A*

This experiment was in part defective since there was an extraneous signal due to hydrogenous material in contact with the bath which complicated the interpretation of the results. However, at the low temperatures the true signal was very large compared with the extraneous signal so that it was possible to correct the data for the extraneous signal with reasonable accuracy. This experiment was important because the crystal was better aligned than in subsequent experiments, lower temperatures were attained, the constant δ in the $T-T^*$ relation was evaluated, and an upper limit for g_{11} was obtained.

Measurements were made alternately at a reference angle of 9.8° and in the direction of $g_{\min}$. A smooth curve was drawn through the points representing the reference angle areas as a function of time. After correction for the extraneous signal, this smoothed curve was used to give the temperature at the reference angle corresponding to the same entropy as that of the measurement for the strong field in the direction of $g_{\min}$. Within the range of this experiment the entropy is given with sufficient accuracy by the $1/T^2$ approximation so that the ratio of temperatures on adiabatic rotation from g_i to g_f is given by

$$\left(\frac{T_f}{T_i}\right)=\left[\frac{(\beta^2H^2/8k^2)g_f^2+b}{(\beta^2H^2/8k^2)g_i^2+b}\right]^{\frac{1}{2}}, \tag{16}$$

where b is the coefficient of $1/T^2$ in the interionic interaction entropy and H is the resonance field. This ratio is independent of temperature. The constant δ in the $T-T^*$ relation, Eq. (15), was determined by insisting that the ratio $T_{9.8°}/T_{0°}$ be a constant independent of the temperature at the reference angle. The constant Δ was taken to be the same as that obtained from ballistic adiabatic susceptibility measurements.[7] A value for δ of $(7\pm2)\times10^{-3}$K° gives the best degree of constancy of $(T_{9.8°}/T_{0°})$. This value is quite reasonable since one finds $\delta=5\times10^{-3}$K° for a spherically symmetrical distribution of protons 5 A from a cerium ion (see Sec. VI a). Some of the detailed results at the lowest temperatures are shown in Table II. At the lowest temperatures T^* and T differ from one another by as much as a factor of 6, so that one sees immediately the inadequacies of NMR as an absolute thermometer in cases where the local rf field differs sub-

stantially from the applied rf field. If the crystal had been ground to a spherical shape, the correspondence between T and T^* would have been considerably better.

Assuming that one has $g_{9.8°}=g_\perp \sin 9.8°$, one can deduce from the experimental data the ratio $(T_{90°}/T_{0°})$ on adiabatic rotation from 90° to 0°. Such average ratios are given in Table III for several average reference angle temperatures. The over-all average of 47.0 for $T_{90°}/T_{0°}$ may be used to calculate an upper limit for $g_{\parallel}$ by solving Eq. (16) with $g_f=g_\perp$, $g_i=g_{\parallel}$, and $H=2.37$ kilogauss. The value of b in Eq. (19) seems to be uncertain, a value $b=3.2\times10^{-6}(\mathrm{K°})^2$ being given by Daniels and Robinson,[12] and a value $b=2.74\times10^{-6}(\mathrm{K°})^2$ given by Hudson.[22] Taking $b=3.2\times10^{-6}(\mathrm{K°})^2$, one finds $g_{\parallel}=0.023$ while for $b=2.74\times10^{-6}(\mathrm{K°})^2$, one finds $g_{\parallel}=0.026$. The actual value of $g_{\parallel}$ will probably be less than the values given above as a result of misalignment. Hence one can deduce from the data only that $g_{\parallel}\lesssim 0.026$.

The initial entropy was $S/R=0.562$. Upon using the experimental results of Daniels and Robinson[12] the lowest temperature expected on adiabatic demagnetization to a field of 2.37 kg is 5.5×10^{-3}°K, a value which may be predicted using the $1/T^2$ law. This temperature compares rather favorably with 5.9×10^{-3}°K calculated from the lowest measured T^*, Table II. However, a rather substantial difference is observed with the expected lowest temperature, 4.5×10^{-3}°K, calculated from Hudson's[22] data. In the last case, the temperature is substantially lower than that calculated using the $1/T^2$ law.

At the very lowest temperatures a substantial absorption of rf energy was observed which no doubt resulted from spin-spin absorption. In addition, at the lowest temperatures a $(30\pm\frac{1}{2})$-cps signal was superposed on the expected signal. The origin of the $(30\pm\frac{1}{2})$-cps signal is not understood.

(c) Experiment *B*

In this experiment there was no detectable extraneous signal. In the helium temperature range, resonances were taken at angles of 0.2°, 3.8°, 18.8°, and 89.8°. At a given temperature the area was independent of angle to within a few percent. The integrated intensity was proportional to $1/T$ within an accuracy of about 3%. There was considerable scatter among the values for 89.8°, and to a somewhat lesser extent also for 18.8°, since the resonances were broader and therefore not as intense as at the smaller angles. No indications of rf saturation were noted even at the lowest temperatures at the highest rf magnetic field employed. However this value of H_1, approximately 2.4×10^{-3} gauss, was still quite small.

TABLE IV. Temperature changes on adiabatic rotations between laboratory angles of 3.8° and 18.8°. T was calculated from T^* by using Eq. (15) with $\Delta=2.5\times10^{-3}$°K and $\delta=7.0\times10^{-3}$°K. All numbers in a row correspond to the same entropy.

$(1/T^*)_{3.8°}$	$(1/T^*)_{18.8°}$	$(1/T)_{3.8°}$	$(1/T)_{18.8°}$	$T_{18.8°}/T_{3.8°}$
58.6	11.10	43.0	10.34	4.16
52.1	9.98	39.4	9.41	4.19
45.7	8.85	35.7	8.45	4.22
39.2	7.72	31.8	7.40	4.30
32.8	6.60	27.5	6.36	4.32
26.3	5.48	22.8	5.16	4.41

[22] R. P. Hudson (unpublished).

TABLE V. Comparison of averaged NMR temperature ratios and expected ratios on adiabatic rotation between angle θ and reference angle θ_{ref}. The experimental temperatures were calculated from the $T-T^*$ relation, Eq. (15), with $\Delta=2.5\times10^{-3}$°K and with $\delta=0$ and $\delta=7.0\times10^{-3}$°K.

θ_{ref} degrees	θ degrees	$T_\theta/T_{\theta\ \mathrm{ref}}$ Expected	$T_\theta/T_{\theta\ \mathrm{ref}}$ Averaged experimental $\delta=0$	$\delta=7\times10^{-3}$°K	Number averaged
3.8	6.2	1.48	1.43	1.41	2
3.8	8.8	2.12	2.28	2.22	5
3.8	11.2	2.69	2.41	2.36	2
3.8	13.8	3.30	3.28	3.19	5
3.8	16.2	3.86	3.15	3.09	2
3.8	18.8	4.45	4.37	4.27	6
3.8	21.2	5.00	4.60	4.47	1
3.8	23.8	5.57	6.07	5.75	2
3.8	28.8	6.65	6.84	6.56	2
18.8	28.8	1.49	1.46	1.43	2
18.8	38.8	1.94	1.87	1.84	2
18.8	58.8	2.33	2.50	2.47	2
18.8	89.8	3.10	2.78	2.77	8

The low-temperature measurements showed that the crystal was not aligned as well as it was in experiment *A* so that no further studies of the value of $g_{\parallel}$ were possible. An estimate of the angle of misalignment, α, gave $\alpha=1.7°$. In this experiment it was possible to assess the general accuracy of the NMR thermometer by comparing temperature ratios on adiabatic rotation with those expected theoretically on the basis of the known properties of the crystal. Measurements were made alternately at some angle and at a reference angle so that effects due to extraneous heat inputs might be compensated. Area ratios were converted to temperature ratios using Eq. (15). A sample of the experimental data is given in Table IV which shows the results of adiabatic rotations between laboratory angles of 3.8° and 18.8° for various values of the temperature at one of the angles. According to Eq. (16) the quantity $T_{18.8°}/T_{3.8°}$ should be a constant. There is a systematic change of the ratio of calculated temperatures which indicates that the $T-T^*$ relation overcorrects the T^* values at low temperatures. The systematic change of $T_{18.8°}/T_{3.8°}$ with temperature, as displayed in Table IV, is characteristic of data at other angles. The systematic change was not so evident when one assumed $\delta=0$ in the $T-T^*$ relation.

Averaged temperature ratios for a number of different angles are shown in Table V. The expected temperature ratios for the 3.8° reference angle were calculated using Eq. (16), and $b=3\times10^{-6}(\mathrm{K°})^2$. The direction of minimum g, which corresponds to laboratory angle of 0°,

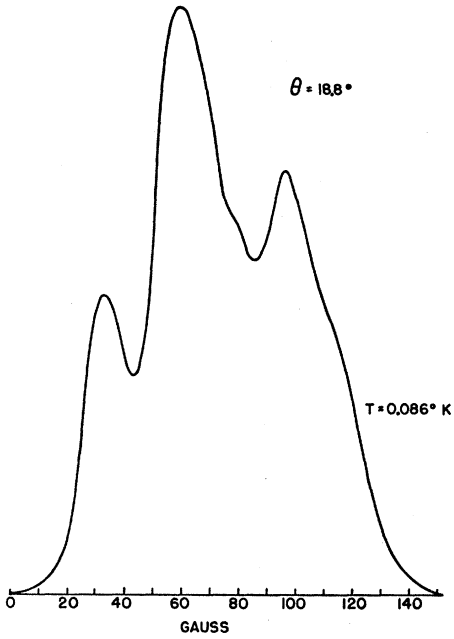

FIG. 3. First integral of phase sensitive detector output for $\theta=18.8°$, $T=0.086°$K, and $\nu=10.921$ Mc/sec. Only relative values of magnetic field are given. The centroid of the structure occurs at the free-proton resonance value.

was determined to an accuracy of 0.1°. In the case of the laboratory angle 3.8°, the g-value was calculated assuming a misalignment of 1.7° and $g_{11}=0.026$. The expected temperature ratios for the 18.8° reference angle were obtained using the ratios of the sines of the angles involved. On the whole the temperature ratios using NMR are in fairly good agreement with the expected values. The measured values are on the average less than the expected ones. The source of the discrepancy lies no doubt in part in errors in the $T-T^*$ relation, but the details are not understood. It should be noted that temperature ratios as inferred from ballistic adiabatic susceptibility measurements were in essential agreement with the expected values once the value of $g_{\min}$ was determined.

The results shown in Table V indicate that so long as local field effects are not excessively large, NMR thermometry should be possible with an accuracy of 5–10%. Under isothermal conditions with small $T-T^*$ corrections the accuracy may be improved to 2–4%. A serious disadvantage of NMR thermometry compared to ballistic susceptibility thermometry is that the form of the $T-T^*$ relation is intrinsically more complicated for the former and the theoretical calculation of the constants in the $T-T^*$ relation requires much detailed information about the crystal.

Another difficulty with NMR thermometry is the rather long time required to take a measurement. This prevents the making of many measurements of the temperature in a short period of time.

The change in temperature, due to the heat leak, during the temperature measurement may hinder a simple interpretation of the result. However, in certain cases NMR thermometry is desirable, e.g., cerium ethyl sulfate, and in many cases the nuclear resonance area provides a useful thermometric parameter.

VI. RESULTS AND DISCUSSION. LINE SHAPES AND RELAXATION TIMES

(a) Line Shapes

The actual experimental data on the structure of the resonance were curves of the output of the phase-sensitive detector as plotted by a recording potentiometer. If the 30-cps magnetic field modulation amplitude is small compared to the line widths, then the output is just the derivative of the absorption curve. If the magnetic field modulation is not small compared to the line widths, the shape of the absorption curve is distorted with no effect on its area.

In general the structure of the resonance was very complicated, with few or no resolved maxima. However, in certain cases maxima were rather well resolved. The curves at $\theta=18.8°$ showed enough resolved structure to make their study fruitful. Figure 3 shows as an example the first integral of the phase-sensitive detector curve for $\theta=18.8°$ and $T=0.086°$K. The centroid of the structure occurs at the free-proton resonance field.

In the experiments of Bloembergen and Poulis[17,18] the proton resonance had structure which resulted from the time-averaged moments of the paramagnetic ions. In this approximation in our experiment a cerium ion produces a dipolar field whose magnitude at the site of a proton depends on the separation of cerium ion and proton and on the orientation of the cerium ion with respect to the line joining the two. If this is the case then the separation of two components of the structure at a fixed angle should have a temperature dependence given by

$$\Delta H \propto \tanh(\beta gH/2kT). \tag{17}$$

Figure 4 shows a plot of ΔH *vs* $\tanh(\beta gH/2kT)$ for the three splittings of Fig. 3. The scatter appears to be mainly a difference between runs rather than within the same run and may be due to scatter in the constant of proportionality between $1/T^*$ and the normalized area. It appears that in our experiments the structure of the resonance line may also be explained by means of the concept of a time-averaged magnetic moment.

A study of the structure of the resonance should also lead to a determination of the cerium-proton distances. However, in these experiments the narrow spectrum and the many nonequivalent proton sites made detailed measurements impossible. Nevertheless one can make a crude estimate of the smallest proton-cerium ion distance by arguing that the two outermost components of the structure should be separated by about $\Delta H=2\bar{\mu}/r^3$. The value of $\bar{\mu}$ is $\frac{1}{2}g_{\perp}\beta\tanh(\beta gH/2kT)$, so that one can equate $(g_{\perp}\beta/r^3)\tanh(\beta gH/2kT)$ to $148\tanh(\beta gH/2kT)$

gauss, the latter being obtained from the largest observed splittings. The smallest value of r thus turns out to be about 5 A. Bleaney, Bowers, and Trenam[23] have concluded from paramagnetic resonance studies of the double nitrates that the rare earth ion is surrounded principally by nitrate radicals and that the divalent ion is surrounded by an octahedron of water molecules. They also state that the divalent ions can occupy either body or face centers of the rare earth ion lattice. The cerium ions lie on a simple rhombohedral lattice.[24] The point at the body center lies 6.92 A from the closest cerium ion whereas a point at a face center lies 5.46 A from the closest cerium ion. Hence if the protons in the octahedron of water molecules surrounding the divalent ion were about 2 A from the divalent ion and if the divalent ion occupied a body center, then the protons would be 5 A or more from the cerium ion. However, if the Mg^{++} ion were at a face center, a 2 A sphere around it would include values of r which were less than 5 A. Hence the possible orientations of water molecules around Mg^{++} ions at face centers might have to be restricted. Since only $\frac{3}{4}$ of the water molecules are around Mg^{++} ions, the remainder of the water molecules must be at other positions suitably far from the Ce^{+++} ions.

(b) Relaxation Times

There are two spin systems in the CMN crystal and one can employ four relaxation times in discussing them. The spin-lattice and spin-spin relaxation times for the paramagnetic spin system will be denoted by τ_1 and τ_2, respectively. The spin-lattice and spin-spin relaxation time for the proton spin system will be denoted by T_1 and T_2, respectively. No information concerning τ_1 could be obtained from the present experiment. The time τ_2 is about 1×10^{-9} sec at 4°K as determined from paramagnetic resonance line widths.[13] Because the structure is produced by the time average magnetic moment of the cerium ions, τ_2 must be less than 10^{-7} sec down to the lowest temperatures obtained.

Similarly an estimate of T_2 for the protons can be obtained from the approximate line width of the NMR components. The line width was about 10 gauss, so that T_2 is about 7.5×10^{-6} sec. Since no indications of rf saturation were detected, $\gamma^2H_1^2T_1T_2$ must be less than one. If one uses the maximum experimental H_1, 0.0024 gauss, and 7.5×10^{-6} sec for T_2, then T_1 must be less than 32 sec. Estimates based on relaxation via the paramagnetic ions[15,16] would give a value 2 or 3 orders of magnitude shorter for T_1, indicating that our power levels were much too small to give saturation.

[23] Bleaney, Bowers, and Trenam, Proc. Roy. Soc. (London) **A228**, 157 (1955).
[24] J. M. Daniels, Proc. Phys. Soc. (London) **A66**, 673 (1953).

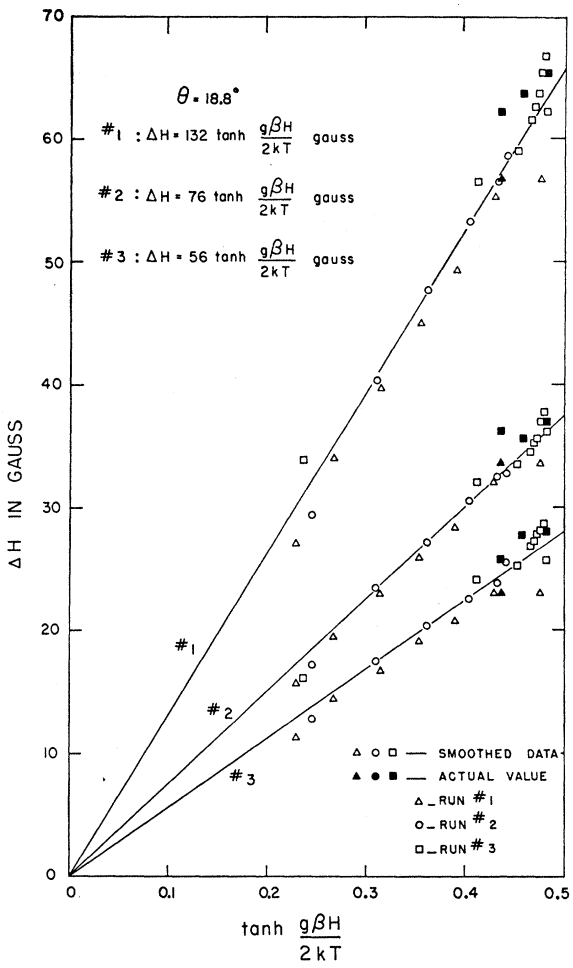

FIG. 4. Splittings between the three pairs of peaks, shown at a particular temperature in Fig. 3, at $\theta=18.8°$ as function of $\tanh(g\beta H/2kT)$.

VII. CONCLUSIONS

The problem of NMR thermometry in paramagnetic crystals at extremely low temperatures is complicated by a number of factors, the most important in CMN being the temperature dependence of the rf magnetic field producing the transitions between nuclear magnetic substates. However, it was possible to account for this temperature dependence fairly well by using a semiempirical method for evaluating the effects of nonspherical crystal shape and the mean square dipolar rf field at a proton resulting from the cerium ions. Upon using this semiempirical method rather good agreement was obtained between the results of the NMR experiments and the results of ballistic adiabatic susceptibility measurements made on the same crystal. In this sense it appears that NMR thermometry may be applied to CMN with an accuracy of 5 to 10% as long as the local field effects are not excessively large. When the local field effects are negligible, an accuracy of about 3% may be obtained.

In studying the structure of the NMR curves at a given angle, one finds that the separation in gauss between any two resolved peaks is proportional to $\tanh(\beta gH/2kT)$ and therefore to the time-averaged cerium magnetization. This means that the spin-spin interaction time for the paramagnetic ions must be shorter than the Larmor period of the protons. The static local fields produced by the time-averaged magnetic moment of the cerium ions vary among the nonequivalent proton sites, so that the external field required by the resonance conditions varies among the sites. The maximum splitting of the resulting structure is rather small compared to the results of Bloembergen and Poulis.[17,18] This can be attributed to a minimum proton-cerium ion distance of about 5 A.

VIII. APPENDIX. COMPUTATION OF THE ABSORPTION CURVE AREAS

The absorption curve areas were computed by numerical double integration as follows. If the recorder curve is considered as a plot of y, the output of the phase-sensitive detector, as a function of x, the coordinate in the direction of the chart feed, the absorption curve is $z=\int_{x_1}^{x} y dx$ *vs* x. The area, u, under the absorption curve is

$$u=\int_{x_1}^{x_2} z dx=\int_{x_1}^{x_2}\left[\int_{x_1}^{x_2} y(x')dx'\right]dx. \qquad \text{(A1)}$$

The integrals z and u can be approximated to any desired degree of accuracy by the sums

$$z_n=\Delta x \sum_{i=1}^{n} y_i, \quad (n\leqslant N) \qquad \text{(A2)}$$

and

$$u=\Delta x \sum_{n=1}^{N} z_n=(\Delta x)^2 \sum_{n=1}^{N}\left(\sum_{i=1}^{n} y_i\right) \qquad \text{(A3)}$$

by taking Δx small enough.

Outside of the region $x_1\leqslant x\leqslant x_2$ one expects to find $y(x)=z(x)=0$ because of the resonance nature of the curves. It is found in practice that $y(x_1)$ and $y(x_2)$ are no larger than the noise. The condition $z(x_1)=0$ holds by definition. However, it is found empirically that $z(x_2)$ is not zero, although it is always much less than the maximum value of z. Hence, it is necessary to correct the value of u for this departure from ideal behavior. Since not all of the causes of this departure are known, it is impossible to derive a rigorous correction. However, when the quantity $\frac{1}{2}(x_2-x_1)z(x_2)=\frac{1}{2}N\Delta x z(x_2)$ is subtracted from u, an area is obtained which is equivalent to averaging the results obtained by integrating first in one sense of x and then in the opposite sense. The correction used considerably reduces the scatter of the areas of curves taken under identical conditions and is exact in correcting for incorrect choice of the line $y=0$. Random processes such as noise and errors in obtaining the y_i's, tend to be canceled by the correction. Effects caused by the change in temperature during the resonance and by too long a time constant in the integrating circuit will also be partially compensated.

ACKNOWLEDGMENTS

We would like to acknowledge the help given to us both in experimental techniques and interpretation of data by Professor C. P. Slichter, Dr. L. C. Hebel, and Dr. J. J. Spokas. We are grateful to Professor C. J. Gorter, with whom we have been able to discuss some of the aspects of this work. We also wish to thank Mr. D. Karmeier for his careful numerical computation of the areas under the absorption curves.

The majority of this work was performed while one of us (T.L.E.) was supported by a fellowship from the Eastman Kodak Company and while another of us (H.R.H., Jr.) was supported by a fellowship from the National Science Foundation.